Continuous Noise Estimation Using Time-Frequency ECG Representation

Piotr Augustyniak

AGH University of Science and Technology, Krakow, Poland

Abstract

Common use of telemedical recordings performed in home care conditions and interpreted automatically justifies the need for a reliable signal-to-noise estimate. We propose new noise measurement technique based on a time-frequency model of noise computed in a quasi-continuous way. The proposed method is dedicated to ECG and uses automatically recognized cardiac components for temporal adaptation of the local bandwidth estimate. This noise is captured in each particular scale as non-uniformly sampled series and next is interpolated to the regions where components of cardiac representation are expected. Our approach yields a quasi-continuous model of the noise with a maximum value of measured to calculated data points ratio. The measurement of the noise level may be specified as temporal function being local ratio of energies from signal and from noise TF zones. The dynamic response of the model to rapid noise changes and thus the temporal precision of the SNR estimation are limited only by the resolution of TF representation. The accuracy of noise estimation for noise model-based and baseline-based methods are similar (0.64dB and 0.69dB respectively) as long as the noise level is stable. However in case of dynamic noise, the proposed algorithm outperforms the baseline-based method (0.95dB and 2.90dB respectively).

1. Introduction

Steadily growing number of ECG recordings gathered in home care or in motion motivates the research for novel methods of noise level assessment. Unavoidable simultaneous activity of adjacent organs (e.g. muscles) and unstable recording conditions (e.g. electrodes contact) distort the signal and raise doubts about diagnostability of the record. In both cases, the noise occurs randomly overlapping the ECG signal in both time and frequency domains. Several noise measurement and removal techniques were proposed in the past including signal averaging [1], adaptive noise canceling [2] or wavelet-based noise reduction [3-7]. Although relying on various principles, these techniques hardly succeed in presence of broadband noise variation and thus are not applicable to home care or moving subject-originating recordings. These methods commonly rely on the baseline as an interval of documented electrical inactivity of the heart when picking a reference value for noise measurement. We dispute this approach, since in real ECG recordings short duration of the baseline limits the noiseprint bandwidth, and rare, irregular occurrence of the baseline limits the contribution of noise measurement points.

An alternative approach presented in this paper consists in recognition of continuous representation of cardiac activity and background electrophysiological components. The identification of these sources is based on coordinates of each particular atom of time-frequency plane in context of the local bandwidth of the electrocardiogram (LBE). Time-frequency atoms found out of the instantaneous ECG bandwidth are classified as noise measurement points and yield a large percentage of values of quasi-continuous noise model. Interpolation or extrapolation was applied for only few gaps when cardiac representation fills all the time-frequency range. The continuous measure of signal-to-noise ratio (SNR) is then calculated as a proportion of energy from cardiac components to the energy from the noise model expressed directly in given temporal confines of time-frequency domain. The LBE is individually adapted to each consecutive heartbeat with use of respectively detected wave borders (fig. 1a). Consequently the method easily adapts to the local variability of background activity, compensates for changes of the heart rate and favorites the measured noise information over the estimates.

2. Classification of time-frequency components

Sampling frequency of 500 or 1000 Hz is commonly used in ECG recordings, but corresponds to the bandwidth of relatively short QRS complex and is significantly overestimated for other cardiac components occupying the majority of record's time. This local oversampling yields a gap above the bandwidth expected for slow cardiac components and the Nyquist frequency. Similarly to the baseline, but significantly longer, these intervals in specified frequency range (scale) don't represent cardiac activity (fig. 1b). Consequently they are suitable to measure the noise level at high frequencies (three upper scales) directly from a scalo-temporal plane.

We found reasonable to correlate the local bandwidth estimate with positions of particular component of the heart cycle (the P, QRS and T waves), because bandwidth within each of these waves depends on different electrical phenomena. Assuming the reliability of wave limits automatically calculated for each heartbeat, the noise measurement intervals are determined in three upper scales in relation to the diagnostic content of the corresponding electrocardiogram.

Several attempts were previously made in our research to determine the local bandwidth of the ECG:

- studies of susceptibility of diagnostic parameters to signal distortion caused by the local random canceling of time-frequency coefficients [8],
- analysis of expert's perception of the ECG trace revealing local signal conspicuity and thus its section-wise relevance to the final diagnosis [9],
- individual assessment of the spectra for optimally-concatenated waves train of selected types [10].

The local bandwidth of the electrocardiogram (LBE) is then a heuristic discrete function $f(n)$ specifying relative bandwidth expected at the time point n:

$$f : \forall n \in \{0,1,...N\} \rightarrow f(n) \in [0;0.5) \qquad (1)$$

This function, using $k_1 ... k_5 \in \{0, 1, ...N\}$ as the representation of standard positions of wave borders is projected to the local positions of current heartbeat wave borders $h_1 ... h_5 \in \{0, 1, ...M\}$ for each point $i = 1...5$ (fig. 1):

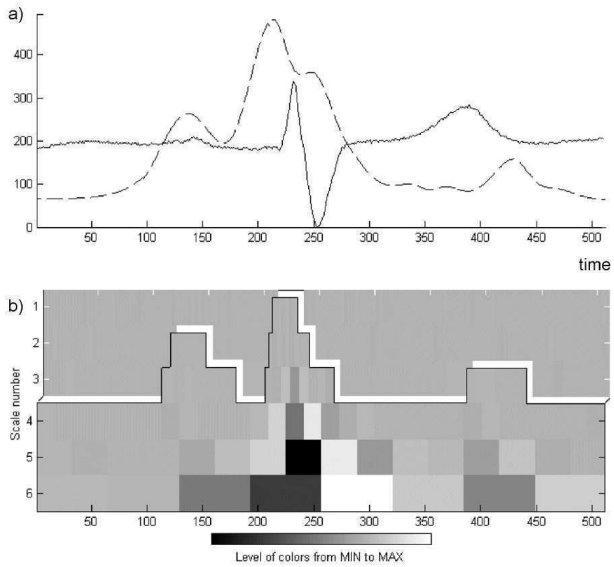

Figure 1. a) The example heartbeat (solid) and the adapted bandwidth variability function (dashed); b) Respective time-frequency signal representation divided in the noise measurement region (above the local cut-off frequency) and the cardiac representation region (below).

$$\forall n \in [k_i, k_{i+1}], \forall m \in [h_i, h_{i+1}] \quad f'(m) = P^{S_i}(f(n)) \qquad (2)$$

with projection scale S_i varying from section to section accordingly to:

$$S_i = \frac{h_{i+1} - h_i}{k_{i+1} - k_i} \qquad (3)$$

The LBE function separates the cardiac and noise components and sets a borderline for seamless measurement of noiseprint. Time-frequency atoms of raw ECG representation are classified as cardiac components only for scale j and time point m satisfying: $f'(m) > 2^{-j-1}$. Otherwise they are classified as extra-cardiac components (noise representation) and included to the running time-frequency model of ECG background activity. The risk of confusion of the noise with the cardiac representation depends on reliability of wave border positions. For each scale, the time-frequency noise model contains as many measured data points as possible and can be updated immediately except for relatively short (in scales 1–3) series of atoms classified as cardiac representation.

3. Seamless measurement of SNR

In the sections filled with expected representation of cardiac activity, the noise level measurement is not performed, and respective values of noise model have to be calculated from the neighboring measured values. Consecutive values of atoms with measured noise in separate scales N_j, $j \in \{1...3\}$, are considered as non-uniformly sampled time series $N_j(\{n, v(n)\})$ and projected to the regular space [11] using the continuous function:

$$S_i(x) = a_i + b_i(x - x_i) + c_i(x - x_i)^2 + d_i(x - x_i)^3 \qquad (4)$$

where $x \in [x_i, x_{i+1}]$, $i \in \{0, 1, ...n-1\}$ best fitted to the time series N_j are known as cubic splines interpolation. Sampling the $S_i(x)$ at the time points m yields the uniform representation of noise, extended to the cardiac component area in three upper scales (fig. 2a):

$$N'_j(m) = \sum_m S_i(x) \cdot \delta(x - mT) \qquad (5)$$

As the scale number increases, the contribution of cardiac representation increases and below the third scale (32 Hz), the bandwidth is continuously occupied by the representation of cardiac activity. Since reliable measurement of noise is not possible in lower frequencies, we extrapolated noise values based on coefficients taken from first three scales. This extrapolation uses second-order polynomials generated by all atoms of embedded trees originating from the considered coefficient:

$$N'(k, j) = a_{k,j} \cdot j^2 + b_{k,j} \cdot j + c_{k,j} \quad (6)$$

The estimation of the noise level at a given time point k on the scale $j > 3$ is based on three values being scale-wise averaged values of atoms $s(n, i)$ of first three scales $M_j(k, i)$ within a corresponding time interval (fig. 2b):

$$M_j(k,i) = \frac{1}{2^{j-1}} \sum_{n=2^{j-i}\cdot k}^{2^{j-i}\cdot(k+1)-1} s(n,i) \quad (7)$$

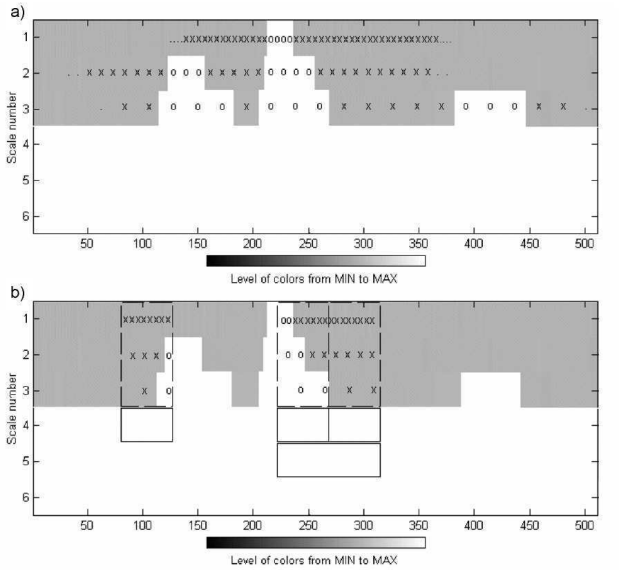

Figure 2. a) Distribution of noise measurement and interpolation samples in first three scales; b) Extrapolation of noise values to low frequency bands with averaging of the noise print in the time domain. Missing values 'o' are estimated from adjacent measured values 'x'.

The final step of the procedure consists in calculating the signal-to-noise ratio (SNR) as a proportion of contribution of energy from time-frequency atoms representing the cardiac activity (below the LBE curve) to the energy represented in quasi-continuous noise model within the same time confines. Length of the temporal window may be adjusted in result of compromise between the flexibility of SNR and bandwidth of considered signal and noise, according to the Heisenberg uncertainty rule. Block diagram of the complete noise measurement procedure is presented in fig. 3.

4. Testing conditions

As a first trial we used stationary (i.e. not modulated) noise patterns and performed two complementary experiments using real signals (with intrinsic noise) and synthesized ECG records (noise-free, but without diagnostically meaningful details).

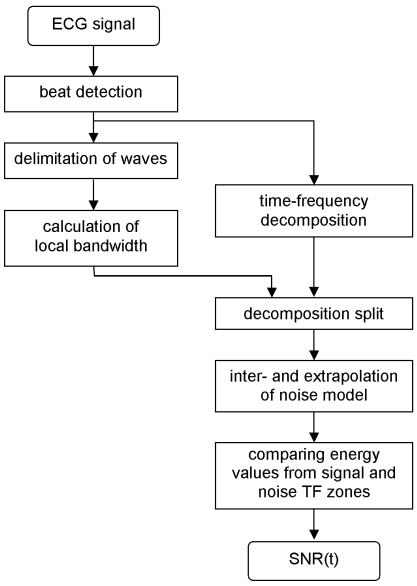

Figure 3. Block diagram of the complete noise measurement procedure.

In all cases, three noise patterns were mixed with the ECG record as representation of common noise sources:

- poor electrode contact (mainly low frequency and abrupt baseline changes),
- electromagnetic interference (mains sinus wave, 60 Hz),
- muscle fibrillation (a clipping-free section was selected)

All noise patterns were taken from the MIT-BIH Database (12 bit, 360 Hz) [12], resampled and mixed with the signal at the following four levels of total energy: 5%, 10%, 20% and 50% (corresponding to –13 dB, –10 dB, –7 dB and –3 dB of signal-to-noise ratio). The artificial records were acquired with use of an ECG recorder (12 bits, 500 Hz) form the test generator (PS450, Fluke) and the real ECG records were taken from the CSE Multilead Database (12 bit, 500 Hz) [13] (fig. 4).

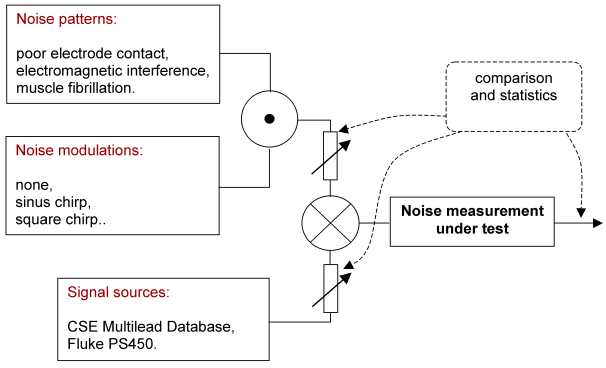

Figure 4. Block diagram of testing procedure.

In the second trial aimed at revealing the dynamic properties of the proposed method, the changes of muscular activity were simulated by the modulation of noise pattern energy with a sine and square waves (chirps) of frequency sweeping from 1 to 10 Hz.

5. Results

Performance of the proposed method for muscular noise measurement was the most interesting result. Accuracy [%] of measured SNR value for different mixing levels is summarized in table 1.

Table 1. Summary of noise measurement accuracy [%] for four mixing levels [dB] of muscular noise pattern.

Signal type	Noise mixing level [dB]			
	-3	-7	-10	-13
CSE database	72	88.5	90	83
synthesized stationary	80	93	92.9	93.4
sinus modulated	78	92	92.2	92.6
square modulated	62	76.5	79	76

Comparison of performance of proposed noise model-based and conventional baseline-based noise measurement methods is presented in figure 5.

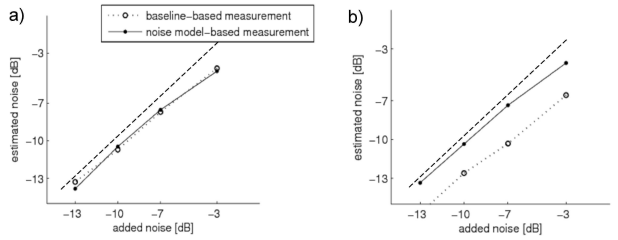

Figure 5. Comparison of noise model-based and baseline-based noise measurement methods, a) static noise, b) sinus modulated noise.

Artificial ECG signals were synthesized mathematically in the generator's low-noise hardware with no measurable random component. The time-frequency representation of the ECG perfectly matches the expected local bandwidth variability. Therefore any difference of estimated and added noise levels is interpreted as SNR-estimator inaccuracy.

A new ECG-dedicated running model-based method for noise estimation was developed and tested. The noise model optimizes the response to the physiological changes of background activity. The accuracy of noise estimation for noise model-based and baseline-based methods are similar (0.64dB and 0.69dB respectively) as long as the noise level is stable. However in case of dynamic noise, the proposed algorithm outperforms the baseline-based method (0.95dB and 2.90dB respectively).

Acknowledgements

Scientific work supported by the Polish State Committee for Scientific Research resources in years 2009-2012 as a research project No. N N518 426736.

References

[1] Moss A, Stern S. Noninvasive Electrocardiology - clinical aspects of Holter monitoring. Saunders Co. London 1996
[2] Akay M. Biomedical signal processing. Academic Press, San Diego, 1994
[3] Akay M. (ed) Wavelets in Biomedical Signal Processing. IEEE Press, New York, 1998
[4] Nikolaev N, Gotchev A. De-noising of ECG signals using wavelet shrinkage with time-frequency dependant threshold. Proc European Signal Processing Conf, EUSIPCO-98 Island of Rhodes, Greece, 2449—2453, 1998
[5] Krishnan S, Rangayyan RM. Automatic de-noising of knee-joint vibration signals using adaptive time-frequency representations. Med Biol Eng Comput 38:2—8, 2000
[6] Paul J, Reedy M, Kumar V. A transform domain SVD filter for suppression of muscle noise artefacts in exercise ECG's. IEEE Trans Biomed Eng 47:645—662, 2000
[7] Nikolaev N, Gotchev A, Egiazarian K, Nikolov Z. Suppression of electromyogram interference on the electrocardiogram by transform domain denoising. Med Biol Eng Comput 39:649—655, 2001
[8] Augustyniak P. Controlling the Distortions Distribution in a Wavelet Packet-Based ECG Compression. International Conference on Image and Signal Processing, Agadir Morroco, 267—277, 2001
[9] Augustyniak P. How a Human Perceives the Electrocardiogram. Computers in Cardiology, 30:601—604, 2003
[10] Augustyniak P. Moving Window Signal Concatenation for Spectral Analysis of ECG Waves. Computing in Cardiology 37:665—668, 2010
[11] Aldroubi A, Feichtinger H. Exact iterative reconstruction algorithm for multivariate irregularly sampled functions in spline-like spaces: the Lp theory. Proc Amer Math Soc 126(9):2677—2686, 1998
[12] Moody GB. The MIT-BIH arrhythmia database CD-ROM. Third Ed., Harvard-MIT Division of Health Sciences and Technology, 1997
[13] Willems JL, Arnaud P, van Bemmel JH. et al. A reference database for multilead electrocardiographic computer measurement programs. Journal of the American College of Cardiology, 6, 1313-1321, 1987

Address for correspondence:

Piotr Augustyniak
AGH University of Science and Technology,
30, Mickiewicz Ave. 30-059 Krakow, Poland
august@agh.edu.pl.